JOURNAL OF MOLECULAR SPECTROSCOPY 167, 375–382 (1994)

Fourier Transform Spectra of Overtone Bands of HCN from 4800 to 9600 cm^{-1}: Some New Transitions of Bending Combination Modes

WOLFGANG QUAPP,* STEFAN KLEE,† GEORG CH. MELLAU,† SIEGHARD ALBERT,† AND ARTHUR MAKI‡

Mathematisches Institut, Universität Leipzig, Augustus-Platz, D-04109 Leipzig, Germany; †Physikalisch-Chemisches Institut, Justus-Liebig-Universität Gießen, Heinrich-Buff-Ring 58, D-35392 Gießen, Germany; and ‡Department of Chemistry, University of Washington, Seattle, Washington 98195

The transition moments and vibration–rotation constants of 18 previously unobserved combination and/or hot bands of $H^{12}C^{14}N$ are reported. Overtone absorption spectra were measured with a Fourier transform interferometer and a multipass absorption cell with a pathlength of up to 352 m. The transition wavenumber measurements were used to derive vibration–rotation constants, and the integrated line intensities were used to derive an estimate of the transition moments. The new transitions are $01^13–01^10$, $11^12–00^00$, $12^02–000$, $32^00–02^00$, $32^20–02^20$, $03^12–01^10$, $03^12–00^00$, $13^11–01^10$, $13^11–00^00$, $13^31–02^20$, $23^30–03^30$, $23^10–03^10$, $23^10–00^00$, $03^12–02^00$, $03^32–02^20$, $14^01–02^00$, $14^21–02^20$, and $04^02–00^00$. © 1994 Academic Press, Inc.

INTRODUCTION

The vibrational and rotational energy level structure of highly excited vibrational states in polyatomic molecules is currently of experimental and theoretical significance. The hydrogen cyanide molecule, HCN, is of fundamental importance to molecular physics, being one of the most studied polyatomic molecules. For HCN and its isotopomers, extensive experimental data of the stretching excitations are available up to relatively high excitation energies (*1*).

Since the higher energy isomer, HNC, is accessible, in principle, through tunneling from high bending vibrations, the manifold of bending vibrations is of particular interest. One of our aims is the shortening of the gap between measured infrared absorption transitions to bending states, and the recently observed very high excited bending states of HCN, which are observed by an emission pumping from above, from electronically excited bent HCN, by Yang *et al.* (*2*). We have been studying the spectrum of HCN in the wavenumber region from 450 up to 10 550 cm^{-1}. In this paper, we report some new transitions to previously unobserved combination states, involving the bending mode ν_2, in the region between 4800 and 9600 cm^{-1}. This region was last measured in 1988 by Smith *et al.* (*3*) and Sasada (*4*). Together with the new results reported here, HCN is probably the molecule with the most extensively characterized vibrational spectrum (next to the also well known CO_2 and N_2O).

The linear HCN molecule has three normal modes, two stretching vibrations of Σ^+ symmetry, and the bending mode of Π symmetry: ν_1 is the CH stretch at 3311.48 cm^{-1}, ν_3 is the CN stretch at 2096.85 cm^{-1}, and ν_2 is the degenerate bending mode at 713.46 cm^{-1}. Some workers use a notation that reverses the role of ν_1 and ν_3 (*3*).

0022-2852/94 $6.00
Copyright © 1994 by Academic Press, Inc.
All rights of reproduction in any form reserved.

EXPERIMENTAL ASPECTS

Hydrogen cyanide of natural isotope content was purified by repeated vacuum distillation. The chemical purity of the sample was checked by its broadband infrared absorption, where only minor contamination by H_2O and CO_2 could be detected.

Fourier transform spectra were recorded in the mid-infrared and near-infrared in the range $1800 \leqslant \tilde{\nu}/\mathrm{cm}^{-1} \leqslant 10\,500$ by means of a Bruker IFS120HR interferometer connected by vacuum transfer optics to a White-type multipass cell of base length 4 m (*5*). This cell, made of stainless steel, allowed for absorption pathlengths of up to 352 m. The experimental conditions of different runs are given in Table I. HCN pressures used in the present experiment were in the range 2.05–3.12 mbar, and were determined by two capacitance gauges (MKS baratron, full scale 10 mbar). The accuracy of the pressure determination is specified to be better than 0.5% of the gauges' reading. All runs were conducted with the cell at room temperature; temperature variations were within the range of ±0.6 K.

The optical components of the present experimental setup were a tungsten lamp with an elevated near-infrared emission as the light source, a Si:CaF_2 beamsplitter, wedged CaF_2 cell windows, gold-coated multireflection mirrors, and a photovoltaic InSb device as the detector. Optical interference filters having a band pass appropriate to the measured range as indicated in Table I were used except in the case of the broadband spectrum (run AM). The unapodized instrumental linewidth was chosen to be less than the Doppler width of HCN at room temperature, again except in run AM.

Each run was calibrated individually since the calibration constant turned out to be strongly dependent on the pathlength adjustment of the multipass cell, even though it was placed between the detector and the interferometer. For calibration of HCN lines we used the wavenumbers for the overtone bands of CO (the 3–0 band for run S, and the 4–0 for run AN). The CO wavenumbers are known to better than ±0.0001 cm^{-1} in heterodyne measurements (*6–8*), and also from more recent heterodyne measurements (*9, 10*). The HCN lines in those two runs were then used to calibrate the other spectra used in this work. For the calibration by linear regression, it was assumed that a single multiplicative factor could be used to calibrate each spectrum, but each spectrum was given a different calibration constant. We believe the absolute accuracy of the measurements is about ±0.0006 cm^{-1}. The absolute uncertainty of each band center (or vibrational energy level) can be estimated by taking the square root of the sum of the calibration uncertainty and the statistical uncertainty.

TABLE I

Parameters of FTIR Measurements of HCN

Run	Date	Range /cm^{-1}	Press. /mbar	Path /m	Resol. /cm^{-1}	scans	Temp. /K	Aper. /mm
AM	9-01-93	1812-10494	2.85	352	0.0306	2500	298.2	1.5
I	5-22-92	4600-5590	4.91	240	0.0098	1200	299.2	1.5
AE	8-10-93	4800-6100	2.83	288	0.0078	399	299.2	1.3
S	5-29-92	5550-6790	3.03	240	0.0118	240	299.2	1.5
AJ	8-24-93	5900-7250	2.70	352	0.0128	1816	297.6	1.5
AI	8-23-93	5900-7250	2.05	160	0.0128	480	298.0	1.5
AN	11-3-93	6900-9300	2.73	128	0.0100	1400	296.0	1.15
AP	11-8-93	8300-10300	2.35	240	0.0167	2650	295.9	1.3

SPECTRUM AND MOLECULAR CONSTANTS OF HCN

Vibrational and Rotational Constants

Systems of lines were sorted into bands with the aid of the Giessen Loomis–Wood program (*11*). The principle of this program is to cut the spectrum into segments of $2B$, where B is the rotational constant, and display many consecutive segments, one above the other, on the monitor of a personal computer. With a good estimate of B, lines belonging to a single subband will appear aligned in a recognizable pattern.

For the assignments, we used predictions given by Maki (*12*), Bowman *et al.* (*13*), and Mills and co-workers (*14*). Estimated constants or constants determined from a preliminary fit were useful in extending the fit to weaker lines and also were useful in verifying the correct assignment. All the identified transitions had relative intensities that were in approximate agreement with the calculated spectrum. No evidence was found for perturbations in the bands reported here. As an example, the transition $11^{1}2$–000 is given in Fig. 1.

Once the lines for a particular upper vibrational level had been identified it was useful to fit them to a simple power series. These preliminary fits were performed using a least-squares fitting procedure with graphical interactive monitoring of the residuals (*15*). The program used for these fits assumed that each subband was a separate vibrational transition with $\delta_{1,l} = 0$ in Eq. (1). The lower state constants were fixed at the known values of these states; cf. Refs. (*3, 4, 12–14*). The results of these preliminary fits are given in Table II. Tables III (for the lower states) and IV (for the upper states) give the results of a more complete fit that combined all the measurements of a particular upper state in a single least-squares fit that took into account the effects of l-type resonance.

For those levels with $v_2 \leq 1$ the energy levels can be represented by the rotational term equation

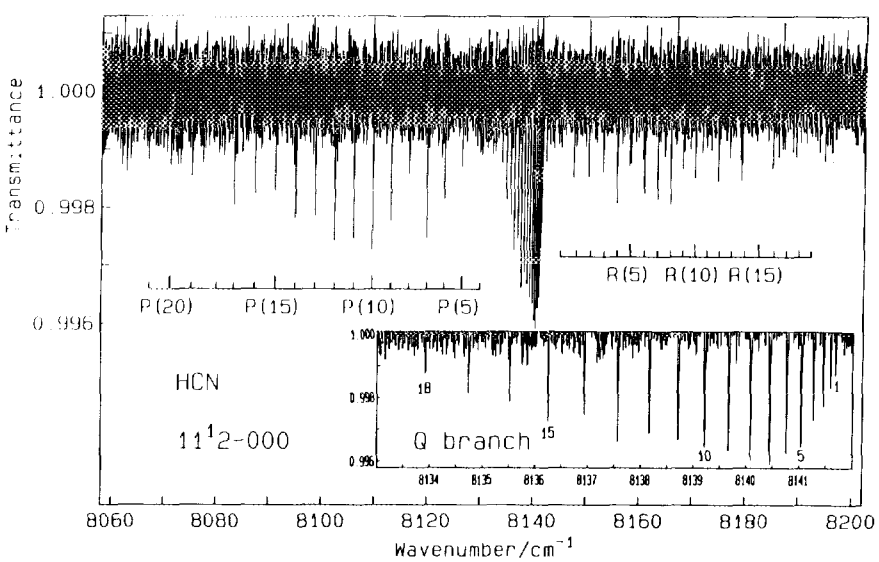

FIG. 1. The band $11^{1e,f}2$–$00^{0}0$ of HCN.

TABLE II

Band Centers, Upper State Power Series Constants (in cm^{-1}), and Transition Moments in Combination Subbands of HCN

Subband	ν_c	B'_{ps} $\times 10^3$	D'_{ps} $\times 10^6$	σ $\times 10^4$	Lines used	μ |Debye $\times 10^5$	Run
$01^{1e}3 \leftarrow 01^{1e}0$	6218.027 0(6)	1.447 27(1)	3.00 (5)	10.6	19	—	S
$01^{1f}3 \leftarrow 01^{1f}0$	6218.027 (1)	1.454 72(2)	2.97 (7)	61.0	15	—	S
$11^{1e}2 \leftarrow 00^{0e}0$	8141.728 (2)	1.447 8(1)	3.2 (5)	25.3	27	4.4(4)	AN
$11^{1f}2 \leftarrow 00^{0e}0$	8141.732 (2)	1.455 39(3)	2.90 (8)	49.8	18	3.45(4)	AN
$12^{0e}2 \leftarrow 00^{0e}0$	8816.004 8(9)	1.455 59(2)	7.17 (5)	24.0	33	6.7(2)	AN
$32^{0e}0 \leftarrow 02^{0e}0$	9510.05 (3)	1.454 4(6)	0.4 (30)	92.0	14	—	AP
$32^{2e,f}0$–$02^{2e,f}0$	9509.074 (7)	1.453 8(2)	0.2 (11)	96.0	17	—	AP
$03^{1e}2 \leftarrow 02^{0e}0$	4856.251 (4)	1.460 88(5)	1.1 (1)	20.2	8	—	I
$03^{1f}2 \leftarrow 02^{0e}0$	4856.251 (1)	1.476 27(3)	1.2 (1)	18.3	11	—	I
$03^{1e}2 \leftarrow 01^{1e}0$	5555.685 7(8)	1.461 01(3)	5.2 (3)	12.0	26	—	AE
$03^{1f}2 \leftarrow 01^{1f}0$	5555.685 8(4)	1.476 251(6)	4.92 (2)	8.1	24	—	AE
$03^{1e}2 \leftarrow 00^{0e}0$	6267.662 (7)	1.461 2(2)	5.69 (4)	47.3	6	—	S
$03^{3e,f}2$–$02^{2e,f}0$	4869.986 (1)	1.467 03(5)	[3.0]	10.4	4	—	I
$03^{3e}2 \leftarrow 02^{2f}0$	4869.983 (3)	1.467 03(5)	2.0 (2)	28.8	7	—	I
$13^{1f}1 \leftarrow 02^{0e}0$	6029.069 1(7)	1.477 55(1)	1.33 (4)	12.0	13	—	S
$13^{1e}1 \leftarrow 01^{1e}0$	6728.502 5(2)	1.461 685(3)	4.39 (2)	4.88	39	—	AI
$13^{1f}1 \leftarrow 01^{1f}0$	6728.500 2(2)	1.477 551(4)	5.08 (2)	6.30	41	—	AI
$13^{1e}1 \leftarrow 00^{0e}0$	7440.479 (1)	1.461 70(2)	4.43 (6)	24.0	43	6.8(6)	AM
$13^{3e}1 \leftarrow 02^{2f}0$	6043.35(2)	1.468 1(2)	2.2 (5)	18.9	7	—	S
$13^{3f}1 \leftarrow 02^{2e}0$	6043.39(2)	1.467 7(2)	4.7 (5)	22.4	5	—	S
$13^{3e,f}1$–$02^{2e,f}0$	6043.371(1)	1.467 90(6)	2.8 (7)	8.57	7	—	S
$23^{3e,f}0$–$03^{3e,f}0$	6401.821 4(3)	1.468 047(5)	3.09 (2)	8.4	23	—	AJ
$23^30 - 03^30$(Q)	6401.820 (1)	1.468 01(8)	2.8 (13)	5.1	5	—	AJ
$23^{1e}0 \leftarrow 03^{1e}0$	6403.017 6(5)	1.461 73(2)	4.31 (6)	9.0	26	—	AJ
$23^{1f}0 \leftarrow 03^{1f}0$	6403.018 7(7)	1.477 73(3)	5.2(2)	8.4	25	—	AJ
$23^{1f}0 \leftarrow 00^{0e}0$	8516.464 (7)	1.476 4(1)	1.0 (4)	47.0	8	—	AP
$04^{0e}2 \leftarrow 00^{0e}0$	6951.676 (2)	1.472 47(3)	14.6 (1)	27.0	25	4.7(3)	AJ
$14^{0e}1 \leftarrow 02^{0e}0$	6696.549 (7)	1.473 2(3)	15.7 (8)	113.0	22	—	AJ
$14^{2e}1 \leftarrow 02^{2e}0$	6696.18 (2)	1.473 4(4)	-4.3 (13)	130.1	12	—	AJ
$14^{2f}1 \leftarrow 02^{2f}0$	6696.21 (1)	1.473 0(2)	3.1 (6)	59.0	9	—	AJ

$$E(v, J, l) = G_v + B_v[J(J+1) - l^2] \pm \delta_{1,f}\frac{1}{2} q_v^0 J(J+1) - D_v[J(J+1) - l^2]^2 + H_v[J(J+1) - l^2]^3 \quad (1)$$

and

$$q_v^0 = q_v - q_{vJ}J(J+1) + q_{vJJ}J^2(J+1)^2, \quad (2)$$

where J is the quantum number for overall rotational angular momentum, l is the quantum number for vibrational angular momentum (*16*), and E is the vibration-rotation term value or vibration–rotational energy in wavenumber or frequency units. $\delta_{1,f}$ is zero if $l = v_2 = 0$ and 1 if $l = v_2 = 1$. If q_v^0 is given a positive sign, then the upper sign (+) is used to calculate the term value for the f states and the lower sign (−) for the e states, for HCN.

When Eq. (1) is used it is common to define a band origin ν_0 given by

TABLE III

Vibrational Energies and Rotational Constants (in cm^{-1}) for the Ground State and Some Excited Bending Modes in HCN after Correcting for l-Type Resonance

$v_1v_2^lv_3$	$G_v - B_vl^2$	B_v	$D_v \times 10^6$	$H_v \times 10^{12}$	$q_o \times 10^3$	$q_{vJ} \times 10^8$	$q_{vJJ} \times 10^{12}$
00^00	0.0	1.478 221 839(24)[a]	2.910 44(22)	3.337(111)	—	—	—
01^10	711.979 582(28)	1.481 772 768(128)	2.977 87(31)	4.09(14)	7.487 739 8(21)	8.878 9(28)	1.433(39)
02^00	1411.413 386(38)	1.485 828 545(138)	3.055 94(36)	5.23(12)	7.596 318 (297)	9.278 3(319)	1.183(250)[b]
02^20	1426.529 856(34)	1.484 997 730(108)	3.038 58(21)	5.23(12)[c]	—	—	—
03^10	2113.450 502(34)	1.489 575 044(137)	3.126 11(33)	5.14(22)	7.709 257(47)	9.856 (22)	1.33(18)[d]
03^30	2143.760 596(89)	1.487 869 366(340)	3.089 25(46)	5.14(22)[c]	—	—	—

a) The uncertainty in the last digits (twice the estimated standard error) is given in parentheses.
b) The $l, l \pm 4$ coupling constant was fixed at the value $\rho = -0.1076 \times 10^{-7} cm^{-1}$.
c) Constrained to be the same for all values of the l quantum number.
d) Also fit was the $l, l \pm 4$ coupling constant $\rho = -0.1076\,(\pm 0.0028) \times 10^{-7} cm^{-1}$.

$$\nu_0 = G'_v - G''_v, \tag{3}$$

which results in ν_0 values that are displaced more than 5 cm^{-1} from the band center for Δ–Π transitions. So, we prefer to absorb the $-B_vl^2$ into the vibrational term to give $G_v - B_vl^2$. One can define

$$\nu_c = (G'_v - B'_vl'^2) - (G''_v - B''_vl''^2), \tag{4}$$

which is very close to the center of the band as observed in the spectrum. Many papers, such as Ref. (*17*), define ν_0 in such a way as to be the same as our ν_c. In this paper, we report both ν_c and $G_v - B_vl^2$ in Tables II–IV.

When $v_2 > 1$, l-type resonance introduces very large effective centrifugal distortion constants if Eq. (1) is used. This is avoided if the full energy matrix for l-type resonance is used to determine the term values. The appropriate equations were given by Maki and Lide (*17*) and more recently by Preusser and Maki (*18*). In this paper, we have used the full l-type resonance matrix as given in Ref. (*17*) to fit the data. The least-squares program used to obtain the constants in Table IV is a distant relative of the program used for Ref. (*17*) and it has been used extensively in fits of data on OCS and N_2O (*19*).

Not all of the information needed to evaluate the l-type resonance matrix elements was available from the present measurements. For example, to our knowledge, no direct measurements have been made of the levels 12^22, 14^41, 04^22, and 04^42. However, enough measurements on other levels have been made to enable us to estimate the needed constants. Those estimated constants are given in Table IV. Errors in those constants will not have significant effect on the values of G_v or B_v given in Table IV.

The constants resulting from the least-squares fits of the observed transitions are given in Tables III and IV. The constants for the lower states are all better known from other measurements in this work which will be reported in a later publication. Those constants of the lower states were given fixed values in the least-squares fits for the present Table IV. In all cases the higher order constants H_v, q_{vJ}, and q_{vJJ} were fairly well determined for the lower states of the transitions. Rather than set those constants to zero in any unknown upper state of interest, they were estimated by fitting the constants measured for many other states to a power series in the vibrational quantum number. The values assigned to those constants are also given in Table IV.

TABLE IV

Vibrational Energies and Rotational Constants (in cm^{-1}) for HCN after Correcting for l-Type Resonance

$v_1v_2^lv_3$	$G_v - B_vl^2$	B_v	D_v $\times 10^6$	H_v $\times 10^{12}$	q_o $\times 10^3$	q_{vJ} $\times 10^8$	q_{vJJ} $\times 10^{12}$
01^13	6930.037 55(37)[a]	1.450 994 3(47)	2.985(15)	[3.8][b]	7.456(5)	7.3(21)	[1.4]
11^12	8141.731 25(78)	1.451 554(15)	2.990(51)	[4.2]	7.753(5)	[9.7]	[1.9]
12^02	8816.003 50(65)	1.455 618(11)	3.068 (35)	[4.9]	[7.825]	[10.1]	[1.9]
12^22	[8830.341 1]	[1.454 780]	[3.04]	[4.9]			
32^00	10921.447 02(253)	1.454 874(40)	2.763(140)[c]	[5.7]	7.911(102)	[11.7]	[2.9]
32^20	10935.597 79(157)	1.454 083(35)	2.763(140)	[5.7]			
03^12	6267.662 22(21)	1.468 589 3(40)	3.153(15)	[5.3]	7.625 8(24)	7.8(13)	[1.4][c]
03^32	6296.516 92(89)	1.466 936 7(79)	[3.10]	[5.3]			
13^11	7440.477 863(41)	1.469 599 20(39)	3.126 6(7)	[5.7]	7.897 11(24)	10.54(5)	[1.9]
13^31	7469.894 62(50)	1.467 881 0(37)	[3.09]	[5.7]			
23^10	8516.469 20(13)	1.469 729 4(16)	3.103 8(47)	[6.1]	7.956 1(9)	10.72(34)	[2.4]
23^30	8545.580 75(27)	1.468 013 8(38)	3.086(13)	[6.1]			
04^02	6951.683 04(75)	1.472 545 (15)	3.094 (59)	[6.0]	[7.694]	[10.2]	[1.4]
04^22	[6966.238 6]	[1.471 723 9]	[3.20]	[6.0]			
04^42	[7009.712 1]	[1.469 162]	[3.13]	[6.0]			
14^01	8107.969 03(172)	1.473 983 (14)	[3.22]	[6.4]	[8.003]	[11.0]	[1.9]
14^21	8122.728 65(204)	1.473 212 (21)	[3.19]	[6.4]			
14^41	[8167.021 5]	[1.470 489]	[3.11]	[6.4]			

a) The 1-σ uncertainty in the last digits is given in parentheses.
b) Constants enclosed in square brackets were fixed in the analysis.
c) In some cases the constants were required to be the same for all values of l.

In several cases more than one band was used in the least-squares fit for a particular vibrational energy level; for instance, we have included data for the 13^11–02^00, 13^11–01^10, and 13^11–00^00 transitions. In those cases we allowed each set of measurements to determine a separate band center, and then used the measurement that we felt was most accurate to determine the band centers and energy levels as given in the tables. This procedure allowed for small errors in the absolute calibration of each spectrum of about ± 0.005 cm^{-1}. Such calibration errors would not affect the rotational constants, so a single set of rotational constants (for each upper state) was determined from the least-squares fit of all observed transitions.

Intensities

The transition dipole moment, $|\mu|$, for each vibrational transition was calculated from the integrated absorbance of individual rovibrational transitions. The line intensities were determined by applying the INTBAT program developed by Johns (*20*). This program makes a least-squares fit of the lineshape to a Voigt profile that has been convolved with the boxcar instrument function. The program has the capability of determining a pressure broadening parameter but, for the present weak lines, the pressure broadening was fixed at values given by Pine (*21*). As a general rule, each measured point lay within $\pm 0.5\%$ of the fitted lineshape.

From the line intensity, S_m, we determined the transition moment, $|\mu|$, in Debye units by means of the equation

$$|\mu|^2 = \frac{S_m 3hcQ_rQ_vTF}{8\pi^3\nu_m L_m \exp[-(E_r'' + E_v'')/kT](1 - \exp[-\nu_m/kT])273.15nC}, \quad (5)$$

where Q_r and Q_v are the rotational and vibrational partition functions, n is Loschmidt's number, E_r'' and E_v'' are the lower state rotational and vibrational energies, T is the temperature, F is the Herman–Wallis factor (assumed to be $F = 1$ for these bands), L_m is the Hönl–London factor, C is the isotopic abundance of the species being considered (0.98523), and ν_m is the frequency of the line. For this work, we used $Q_v = 1.0676$ and $Q_r = 140.45$ for the 00^00 state. $|\mu|$ is given in Table III for some of the bands. Only a few of the stronger lines were used for the intensity determination.

CONCLUSION

This work demonstrates that overtone absorption measurements still can uncover new electronic ground state levels at high vibrational excitation even for the extensively studied HCN molecule. Thus, the ladder of HCN bending combination states is extended up to near the lower rungs of the ladder represented by recently reported SEP experiments (stimulated emission pumping) beginning with, for example, 8995.2 cm^{-1} for 04^03, by Wodtke and co-workers (*2, 22, 23*). The ladder of energy levels determined by our overtone absorption data already overlaps measurements with a new collisional approach at 8815.97 cm^{-1} for the 12^02 state (*24*).

ACKNOWLEDGMENTS

Some intensity calculations were done by A. Loh. Both AM and WQ thank the personnel of the Giessen Lab for the friendly hospitality. The authors also thank B. P. Winnewisser for comments on the manuscript. The work was possible with financial support of the Deutsche Forschungsgemeinschaft.

RECEIVED: May 5, 1994

REFERENCES

1. D. ROMANINI AND K. K. LEHMANN, *J. Chem. Phys.* **99,** 6287–6301 (1993).
2. X. YANG, C. A. ROGASKI, AND A. M. WODTKE, *J. Opt. Soc. Am. B* **7,** 1835–1850 (1990).
3. A. M. SMITH, S. L. COY, W. KLEMPERER, AND K. K. LEHMANN, *J. Mol. Spectrosc.* **134,** 134–153 (1989).
4. H. SASADA, *J. Chem. Phys.* **88,** 767–777 (1988).
5. K. A. KEPPLER, XII. Colloq. on High Resolution Spectroscopy, paper L4, Dobris, 1992; XIII. Colloq. on High Resolution Spectroscopy, poster H5, Riccione, 1993.
6. C. R. POLLOCK, F. R. PETERSEN, D. A. JENNINGS, J. S. WELLS, AND A. G. MAKI, *J. Mol. Spectrosc.* **99,** 359–368 (1983).
7. A. G. MAKI, J. S. WELLS, AND D. A. JENNINGS, *J. Mol. Spectrosc.* **144,** 224–229 (1990).
8. T. GEORGE, B. WU, M. DAX, M. SCHNEIDER, AND W. URBAN, *Appl. Phys. B* **53,** 330–332 (1991).
9. F. STROH AND KEN EVENSTON, personal communication, NIST, Boulder, 1993.
10. T. GEORGE, PhD. dissertation, Institut für Angewandte Physik, Universität Bonn, 1993.
11. B. P. WINNEWISSER, J. REINSTÄDTLER, K. M. T. YAMADA, AND J. BEHREND, *J. Mol. Spectrosc.* **136,** 12–16 (1989). F. STROH, J. REINSTÄDTLER, J. C. GRECU, AND S. ALBERT, "The Giessen Loomis–Wood Program LW 5.1," Justus-Liebig-Universität Giessen, 1992. [Unpublished].
12. A. G. MAKI, *J. Appl. Phys.* **49,** 7–11 (1978).
13. J. M. BOWMAN, B. GAZDY, J. A. BENTLY, T. J. LEE, AND C. E. DATEO, *J. Chem. Phys.* **99,** 308–323 (1993).
14. S. CARTER, I. M. MILLS, AND N. C. HANDY, *J. Chem. Phys.* **99,** 4379–4390 (1993).
15. F. STROH, personal communication, 1992.
16. W. QUAPP AND B. P. WINNEWISSER, *J. Math. Chem.* **14,** 259–285 (1993).

17. A. G. MAKI AND D. R. LIDE, *J. Chem. Phys.* **47,** 3206–3219 (1967).
18. J. PREUSSER AND A. G. MAKI, *J. Mol. Spectrosc.* **162,** 484–497 (1993).
19. A. G. MAKI AND J. S. WELLS, "Wavenumber Calibration Tables from Heterodyne Frequency Measurements," NIST Special Publication 821, U.S. Government Printing Office, Washington, DC, 1991.
20. J. W. C. JOHNS, *Mikrochim. Acta* [*Wien*] **111,** 171–188 (1987); private communication.
21. A. S. PINE, *J. Quant. Spectrosc. Radiat. Transfer* **50,** 149–166 (1993).
22. X. YANG, C. A. ROGASKI, AND A. M. WODTKE, *J. Chem. Phys.* **92,** 2111–2113 (1990); X. YANG AND A. M. WODTKE, *J. Chem. Phys.* **93,** 3723–3724 (1990).
23. D. M. JONAS, X. YANG, AND A. M. WODTKE, *J. Chem. Phys.* **97,** 2284–2298 (1992).
24. J. S. BASKIN, A. SAURY, AND E. CARRASQUILLO, M., *Chem. Phys. Lett.* **214,** 257–264 (1993); A. SAURY, J. WU, AND E. CARRASQUILLO M., *J. Mol. Spectrosc.* **164,** 416–424 (1993).